Mitochondrial Structure and Polarity in Dendrites and the Axon Initial Segment are Regulated by Homeostatic Plasticity and Dysregulated in Fragile X Syndrome

Pernille Bülow
Emory University https://orcid.org/0000-0003-1884-6189
Peter A Wenner
Emory University
Victor Faundez
Emory University
Gary J Bassell (gary.bassell@emory.edu)
Emory University

Short report

Keywords: FMR1, FMRP, mitochondria, homeostatic plasticity, compartment-specific, dendrite, axon initial segment

Posted Date: February 2nd, 2021

DOI: https://doi.org/10.21203/rs.3.rs-158378/v1

Mitochondrial Structure and Polarity in Dendrites and the Axon Initial Segment are Regulated by Homeostatic Plasticity and Dysregulated in Fragile X Syndrome

Pernille Bülow[1], Peter A. Wenner*[2], Victor Faundez*[1], Gary J. Bassell[1]*[#].

Departments of Cell Biology[1] and Physiology[2]. Emory University School of Medicine. Atlanta. GA 30322

*co-corresponding authors

[#]lead-contact: Gary J. Bassell

gary.bassell@emory.edu

Abstract

Mitochondrial dysfunction has long been overlooked in neurodevelopmental disorders, but recent studies have provided new links to genetic forms of autism, including Rett syndrome and Fragile X Syndrome (FXS). In parallel, recent studies have uncovered important basic functions of mitochondria to power protein synthesis, synaptic plasticity and neuronal maturation. The mitochondrion also responds to neuronal activity by altering its morphology and function, and this plasticity of the mitochondrion appear important for proper neuronal plasticity. Previous research has reported disease induced changes in mitochondrial morphology and function, but it remains unknown how such abnormalities affect the ability of mitochondria to express activity dependent plasticity. This study addresses this gap in knowledge using a mouse model of FXS. We previously reported abnormalities in one type of homeostatic plasticity, called homeostatic intrinsic plasticity, which is known to involve structural changes in the axon initial segment (AIS). Another form of homeostatic plasticity, called synaptic scaling, which involves postsynaptic changes in dendrites, is also impaired in FXS. It remains unknown if or how homeostatic plasticity affects mitochondria in axons and/or dendrites and whether impairments occur in neurodevelopmental disorders. Here, we test the hypothesis that mitochondria are structurally and functionally modified in a compartment specific manner during homeostatic plasticity in cortical neurons from wild type mice, and that this plasticity-induced regulation is altered in Fmr1 KO neurons, as a model of FXS. We uncovered dendritic specific regulation of mitochondrial surface area, whereas AIS mitochondria show changes in polarity; both responses are lost in Fmr1 KO. Taken together our results demonstrate impairments in mitochondrial plasticity in FXS, which has not previously been reported. These results suggest that mitochondrial dysregulation in FXS contributes to abnormal neuronal plasticity, with broader implications to other neurodevelopmental disorders and therapeutic strategies.

Keywords (3-10):

FMR1, FMRP, mitochondria, homeostatic plasticity, compartment-specific, dendrite, axon initial segment

Introduction

Mitochondria are essential for regulating cellular metabolism and maintaining neuronal health and abnormal mitochondrial function is associated with altered neuronal development and disease (Valenti et al., 2014). More recently, studies have demonstrated impairments in mitochondrial structure and function in various neurodevelopmental mouse models of autism, including Fragile X Syndrome (FXS). Mitochondria are fragmented and depolarized in neurites of the FXS mouse model, the Fmr1 knock out (KO), and the *Drosophila*, *dFmr1* (Shen et al., 2019; Weisz et al., 2018). Thus, restoring mitochondria function is an exciting path for future therapeutic strategies. However, we still do not know how these impairments in mitochondrial structure/function contribute to symptoms in disease.

FXS is characterized by intellectual disability, sensory hypersensitivities and seizures. Moreover, the mutation causing FXS is one of the leading monogenic causes of autism. One of the core phenotypes in FXS animal models is abnormal synaptic, structural and functional plasticity (Bulow et al., 2019; Huber et al., 2002; Meredith et al., 2007; Soden and Chen, 2010). We recently reported cell-type specific abnormalities in homeostatic intrinsic plasticity (HIP) in Fmr1 KO neurons, where some cells displayed exaggerated HIP while HIP was absent in others (Bulow et al., 2019). HIP is critical for maintaining neuronal activity levels by regulating the intrinsic membrane excitability of neuronal membranes. Another form of homeostatic plasticity is called synaptic scaling, which regulates neuronal activity by altering postsynaptic strength. One group found that synaptic scaling is absent in hippocampal Fmr1 KO neurons (Soden and Chen, 2010). While HIP mainly regulates intrinsic excitability by altering ion channel expression/function at the axon initial segment, synaptic scaling solely regulates postsynaptic strength in the dendrites. Thus, Fmr1 KO neurons display compartment specific abnormalities in distinct forms of homeostatic plasticity.

Interestingly, a number of studies have demonstrated that mitochondria may support neuronal plasticity in dendrites and axons (Kuzniewska et al., 2020; Rangaraju et al., 2019). Moreover, studies have reported morphological changes in mitochondria in response to neuronal plasticity (Chang et al., 2006; Li et al., 2004). Specifically, dendritic residing mitochondria become larger after activity silencing, but fragmented following

activity increase (Chang and Reynolds, 2006; Li et al., 2004). Currently, it remains unknown how mitochondrial shape/function is regulated at the molecular level during activity. We know that the synthesis of nuclear encoded mitochondrial protein is upregulated during a chemical LTP paradigm in synaptoneurosomes (Kuzniewska et al., 2020), and the incorporation of these proteins into the mitochondrion appear necessary for synaptic plasticity. FMRP, the protein lost in FXS, is best known as a translational repressor, and FMRP targets ~1.4% of all mitochondrial annotated mRNAs (Rath et al., 2021; Richter et al., 2015; Suhl et al., 2014). Upon changes in neuronal activity, FMRP derepresses its mRNA targets allowing for translation and upregulation (Muddashetty et al., 2011). FMRP may regulate the translation of mitochondrial proteins in an activity dependent manner or alternatively the effect on mitochondria may be downstream of the effect of FMRP on protein synthesis. Here we test the hypothesis that loss of FMRP impairs mitochondrial plasticity. To date, it remains completely unknown if and how defects in mitochondria structure/function in Fmr1 KO neurons impairs neuronal plasticity. Specifically, we address how the Fmr1 mutation causing FXS affects mitochondrial plasticity during a homeostatic plasticity paradigm.

HIP and other forms of homeostatic plasticity are expressed in compartment specific manners but are both protein synthesis dependent (Muraro et al., 2008; Sutton et al., 2006). HIP is typically associated with changes in the axon initial segment (AIS) (Grubb and Burrone, 2010; Kuba et al., 2010), while synaptic scaling, a type of homeostatic plasticity which regulates synaptic strength, exclusively occurs on postsynaptic spines in dendrites (Sutton et al., 2006; Turrigiano et al., 1998). Thus, the same activity perturbation (e.g. activity deprivation) can trigger multiple types of homeostatic mechanisms that express in distinct neuronal compartments. Previously, most work has focused on how mitochondria are regulated by activity in dendrites (Chang et al., 2006; Kuzniewska et al., 2020; Li et al., 2004). However, the axon, and particularly the AIS, is essential for regulating neuronal excitability and understanding how the mitochondrion contributes to plasticity at the AIS may be especially important for dysregulated excitability in many models of FXS and ASD (Contractor et al., 2015). Therefore, we tested the hypothesis that activity perturbation triggers compartmentalized changes in the mitochondrion structure and function, and that this mitochondrial plasticity is altered in Fmr1 KO neurons.

Results and discussion

We previously triggered homeostatic plasticity in days in vitro (DIV) 12 WT and Fmr1 KO cortical primary neurons by co-applying TTX and APV for 48 hours (Bulow et al., 2019). This treatment is often used to trigger protein synthesis dependent forms of homeostatic plasticity (Soden and Chen, 2010; Sutton et al., 2006). After 48 hours of treatment, we performed immunocytochemistry to visualize the mitochondria morphology in dendrites and the axon initial segment (AIS) (Figure 1). In another set of experiments, we tested compartmental changes in mitochondrial function by performing live-cell imaging to visualize the mitochondrial membrane potential in dendrites or the AIS (Figure 2). In general, we quantified larger and more numerous mitochondria in the dendrite compared to the AIS (Fig 1), consistent with previous literature describing differences between mitochondria in dendrites and axons (Chang et al., 2006). In accordance with our hypothesis, we observed compartment specific changes in the mitochondrial morphology and membrane potential (also referred to as the "polarity") in wild-type (WT) neurons. Specifically, after TTX/APV, WT neurons displayed a unique increase in the surface area of dendritic-residing mitochondria but not in mitochondria within the AIS (Fig 1). Conversely, the mitochondrial polarity was distinctly reduced in AIS-residing mitochondria,but not in mitochondria within the dendrite (Fig 2). Thus, 48-hour activity deprivation led to compartment specific changes in the morphology and polarity of mitochondria in WT neurons. We hypothesize that these compartment specific changes support the expression of distinct types of homeostatic plasticity. For example, we speculate that the morphological changes in dendritic-residing mitochondria suggests changes in functional activity of the mitochondria that could support synaptic plasticity. Alternatively, synaptic scaling may trigger downstream mechanisms that lead to enlargement of the mitochondria, perhaps to maintain the increased synaptic size that occurs during synaptic scaling. Both of these speculations could account for the mitochondrial contributions to synaptic/structural plasticity observed in recent papers (Kuzniewska et al., 2020; Rangaraju et al., 2019), and it raises the interesting possibility that absence of mitochondrial plasticity impairs the process of synaptic scaling or the maintenance of stronger synapses in the Fmr1 KO. In contrast, we speculate that reduced polarity of AIS-residing mitochondria after TTX/APV affects mitochondrial buffering of intracellular Ca^{++}. A reduced membrane potential can suggest

uncoupling of the mitochondrial electron transport chain (ETC) which could impair mitochondrial Ca^{++} buffering or, alternatively, increased Ca^{++} entry into the mitochondria. Ca^{++} signaling is critical for the expression of homeostatic plasticity, including HIP (Lee et al., 2015), and reduced or increased intracellular Ca^{++} could influence pathways regulated by neuronal activity. Alternatively, the membrane potential reduction of the AIS-mitochondria may be a consequence of the expression of HIP. Irrespective of the directionality of the changes we observe in mitochondria, our study measures an intriguing correlation between compartmentalized changes in mitochondrial morphology/function and the expression of distinct types of homeostatic plasticity (Bulow et al., 2019).

Consistent with previous reports, we quantified alterations in both the morphology and membrane potential of Fmr1 KO neurons at baseline. In dendrites, mitochondria had a larger surface area, while mitochondria were longer in the AIS of Fmr1 KO neurons (Fig 1). This increase in mitochondrial size contrasts with previous studies reporting smaller and rounder mitochondria in animal models of FXS (Shen et al., 2019; Weisz et al., 2018), although one study using human neurons found no differences in mitochondrial morphology between patient cells and controls (Nobile et al., 2020). There are several possibilities that could account for the discrepancy in our results compared to others: 1. the increased size may represent mitochondrial "swelling", which is a phenotype typically associated with dysfunctional mitochondria. 2. The mitochondria observed may represent "clumps" of fragmented mitochondria. While this is possible, our technical approach to measure mitochondrial morphology is similar to previous studies (Shen et al., 2019) thereby supporting the soundness of our finding. 3. Previous studies have used *dFmr1* flies (Weisz et al., 2018) or Fmr1 KO adult hippocampal stem cells (Shen et al., 2019) to assess mitochondrial morphology. Our study uses DIV 12 cortical primary neurons which likely represent a distinct developmental time point of brain development. Mitochondria shape and function changes during brain development (Khacho et al., 2016) and we hypothesize that defects in mitochondrial morphology in FXS are developmentally regulated. In contrast with the enlarged (rather than the typically fragmented size of Fmr1 KO mitochondria, we did measure reductions in the membrane polarity of both dendritic- and AIS-residing mitochondria (Fig 2), which is a result consistent with previous reports (Licznerski et al., 2020; Shen et al., 2019).

A main finding of our study is that Fmr1 KO neurons lack mitochondrial plasticity. We speculate that the loss of mitochondrial plasticity may contribute to or be a result of abnormal homeostatic plasticity expression. We noticed that the Fmr1 KO AIS-residing mitochondria did display a small decrease in membrane potential after TTX/APV, but this difference was a fraction of the observed reduction in the WT (Fig 2). Moreover, after TTX/APV, WT and KO mitochondria in the AIS no longer differed in polarity. On the other hand, dendritic-mitochondria displayed no further enlargement after TTX/APV in the Fmr1 KO neurons (Fig 1). In sum, Fmr1 KO mitochondria display an insensitivity to neuronal activity in both dendrites and AIS. We hypothesize that FMRP regulates mitochondrial morphology and polarity in an activity-dependent manner, and that loss of FMRP impairs this process. It is possible that mitochondrial plasticity is absent in Fmr1 KO neurons because the mitochondria are already phenocopying WT mitochondria during plasticity. This idea aligns with previous work suggesting that FMRP primarily is an activity sensitive molecule which plays a critical role in mediating molecular pathways during plasticity (Niere et al., 2012; Osterweil et al., 2010). We hypothesize that abnormal mitochondrial plasticity impairs the expression of HIP in Fmr1 KO neurons previously reported by our lab (Bulow et al., 2019).

In summary, our work confirms our hypothesis that mitochondria structure and function are regulated in compartment specific manners during homeostatic plasticity in WT neurons, but absent in Fmr1 KO mitochondria. Mitochondrial abnormalities at baseline may be directly or indirectly caused by loss of FMRP expression. Further work is necessary to understand the underlying molecular mechanism of how FMRP regulates mitochondrial plasticity, when mitochondrial defects arise in FXS, and lastly how restoring mitochondrial plasticity can rescue neuronal plasticity.

Limitations

We consider two limitations to our study. First, we use neurons from postnatal day 1 mice that are cultured for 12 days. We know that the expression of mitochondrial shape/function changes with development, and so may mitochondrial plasticity. However, since we are replicating results from previous work using other cell types/ages,

we expect that our observations of mitochondrial plasticity are relevant across multiple model systems. A second limitation is that while this work uncovers novel aspects of mitochondria plasticity in wild type and Fmr1 KO neurons, we do not know the underlying molecular mechanisms. We hypothesize that mitochondrial plasticity is protein synthesis- and FMRP-dependent. Future studies will need to address these exciting ideas.

List of abbreviations

FXS - Fragile X Syndrome, HIP - Homeostatic intrinsic plasticity, AIS - Axon initial segment, FMRP - Fragile X Mental Retardation Protein, ATP - adenosine triphosphate, WT - wild type, KO - knock out, LTP – long term potentiation, DIV – days in vitro

Methods

Mice: *FMR1*^{HET} females (backcrossed on C57BL6 background, B6.129P2-Fmr1tm1Cgr/J Stock No: 003025) were crossed with WT C57BL6 males (Jackson Laboratory) to generate litters of pups with mixed genotypes (*Fmr1*$^{-/y}$, Fmr1^{HET} or wild-type (WT)). Thus, for all experiments, *Fmr1*$^{-/y}$ male pups were compared to their WT littermate control. We performed PCR to identify genotypes on postnatal day 0 – 1 (P0-P1) as described previously. The mice were housed in a 12 hr light/dark cycle and the animal protocol was approved by the Institutional Animal Care and Use Committees at Emory University.

Primary cortical neuronal cultures: Cerebral cortices were dissected and cultured from genotyped wild type and Fmr1 *Fmr1*$^{-/y}$ pups on P0-P1. The cortices were enzymatically dissociated using trypsin (Thermo Fisher Scientific; 10 min), mechanically dissociated in Minimum Essential Media (MEM; Fisher) supplemented with 10% Fetal Bovine Serum (FBS; Hyclone) and stained to assess viability using Trypan Blue (Sigma). The neurons were plated in one of 2 ways: For immunocytochemical experiments, the neurons were plated on coverslips (Matsunami Inc., 22mm) coated with FBS, poly-l-lysine and laminin. A total of 35,000 neurons were plated as a 'spot' on the center of the coverslip to create a small, high density network.For live cell imaging, 100K neurons were plated on 35 mm Glass Bottom MatTek petri-dishes (MatTek Corp., Cat no: P35G-1.5-14-C) coated with

FBS (Gibco), poly-lysine (Sigma) and laminin (Sigma). The neurons were cultured in standard growth medium (glial conditioned neurobasal (Fisher) supplemented with glutamax (Gibco) and B27 (Invitrogen)), and half of the media was exchanged 2-3 times a week until experimental treatments began. No antibiotics or antimycotics were used. The cultures were maintained in an incubator regulated at 37 C, 5% CO_2 and 95% relative humidity. Culturing protocol is similar to Bülow et al. (Bulow et al., 2019). All experiments were performed with days *in vitro* (DIV) 12 neuronal cultures.

Pharmacology: Drugs were used in the following concentrations (in μM): TTX, 1 (Tocris); APV, 100 (Tocris). Drugs were added to fresh standard growth medium and added to the cultures by a complete media change on Day *in vitro* (DIV) 10 and lasted for 48 hours. The treatment drugs were refreshed after 24 hours. Control cultures had a simultaneous complete media change but without drugs. Cultures were randomly assigned to each treatment group (control, TTX/APV). All experiments occurred on DIV 12.

Immunocytochemistry of mitochondrial morphology and AIS colocalization: The coverslips were washed once with 37ºC in phosphate buffered saline (PBS), and fixed with 37ºC 4% paraformaldehyde (mixed with PBS) for 15 min at 37ºC. The cultures were washed 3 times, permeabilized with 0.2% Triton in 1x PBS for 10 min at room temperature (RT), washed with 20%/0.15% Tris (Corning, cat no:46-030-CM)-Glycine (Sigma, cat no: 8001) in 1x PBS for 5 min, and blocked for 1 hour in a 5% Bovine Serum Albumin (Roche Diagnostics, cat no: 03116964001) solution. The coverslips were incubated with the primary antibodies overnight at 4ºC, washed 3 times, incubated with secondary antibodies for 1 hr at RT, washed 3 times and mounted. All imaging occurred within the first week after mounting.

Primary antibodies: Hsp60 (D6F1), Cell signaling (Cat no: 12165S), Ankyrin G, NeuroMabs (Cat no: 75-146), MAP2, Synaptic Systems (Cat no: 188-004); Neurofascin, Cell Signaling (cat no: 15034).

Secondary antibodies: Alexa Fluor 488, Life Technologies (Cat no: A21206), IgG Cy3, Jackson ImmunoResearch (Cat no: 715-165-150), Cy5-Affinipure, Jackson ImmunoResearch (Cat no: 715-175-150).

All antibodies were used at 1:500 dilution.

Imaging, image processing and imaging analysis of mitochondrial morphology and AIS colocalization: Imaging was performed on a Nikon Eclipse Ti-E inverted microscope with Z-stacks measuring 0.2 um steps (around 10 total steps) with a 60X magnification lens. The images were deconvoluted with Autoquant X3.1 Software and analyzed in ImageJ/FIJI (version 2.0.0-rc-69/1.52n) using the plug in "Mito-Image J" (Wiemerslage and Lee, 2016). Each neuron had the following compartments outlined: soma, dendrite (15 um away from the soma, 15 um in length, 3-4 dendrites were analyzed per neuron), axon initial segment (defined as described by Evans et al. (Evans et al., 2013). For the mitochondria stain, we picked the 3 stacks in best focus and converted these into a max intensity projection. The mitochondria channel was thresholded automatically using the thresholding program "IsoData". All mitochondria detected by the program were confirmed by eye.

TMRM live-cell imaging: TMRM was acquired from ThermoFisher Scientific (Cat no: T668), and diluted to 10 nm in fresh cell culture medium. The TMRM medium was applied to the cell cultures for 20 min at 37ºC. The cultures were washed once in warmed imaging buffer (137 mM NaCl, 0.56 mM MgCl, 4.7 mM KCl, 1.28 mM CaCl, 1.28 mM glucose, 1 mM NaPO4, 10 mM Hepes. Oxyfluor (Milipore, SAE0059) was added on the day of imaging). The live cell Imaging was performed on a Nikon TE2000 inverted microscope with a 60X magnification lens at 37ºC, and the imaging session lasted maximally 30 min.

To identify the axon initial segment, we first incubated the cell cultures with a primary antibody against the extracellular domain of Neurofascin (Cell Signaling, cat no: 15034, 1:500) for 5 min at 37ºC. We washed twice with fresh culture medium, added a secondary antibody (Alexa Fluor 488, Life Technologies (Cat no: A21206)) for 1 min at RT in the dark, and then washed once with fresh cell culture medium and added the TMRM medium (10 nm) and followed the protocol described for the neurites.

The TTX/APV treated cultures had TTX/APV added to the incubation medium at all steps.

FCCP (0.5 uM) (Carbonyl cyanide-4-(trifluoromethoxy)phenylhydrazone) (FCCP Sigma Cat# C2920) was added 5 minutes into recordings.

Image analysis of TMRM intensity: The images were analyzed in FIJI. The dendritic region of interest was defined as 15 um away from the soma and 15 um in length. 2-4 dendrites were analyzed per cell. The AIS

was outlined based on the co-labeled neurofascin stain. The area and mean intensity of the ROIs were quantified in FIJI.

Statistics and Biological Replicates: The morphology and TMRM intensity data sets were evaluated using the Kolmogrov-Smirnov statistical test followed by Bonferroni corrections (alpha = 0.05). All p-values are listed in the figures. Experiments for mitochondrial morphology (Figure 1) were repeated in three independent experiments. Experiments for mitochondrial membrane polarity (Figure 2) were repeated in three independent experiments for mitochondria in the dendrites. For the AIS, experiments were repeated in four independent experiments comparing WT and Fmr1 KO neurons. WT cultures were repeated an extra time without a Fmr1 KO comparison, leading to a total of five independent biological replicates for the WT, and four independent biological replicates for the Fmr1 KO.

Declarations:

Funding: This work was supported by NIH grants 1R01MH109026 (GJB), R01NS065992 (PAW), 1R56MH111459 and 1RF1AG060285 (VF).

Conflict of interest statement: There are no interests to declare by all authors

Ethics approval and consent to participate: Not applicable

Consent for publication: Not applicable

Availability of data and materials: Please contact author for data requests

Author Contributions: PB, GJB, PAW and VF conceived of the experimental design. PB completed all experiments. PB, VF and GJB prepared the manuscript and figures.

Acknowledgements: Not applicable

References

Bulow, P., Murphy, T.J., Bassell, G.J., and Wenner, P. (2019). Homeostatic Intrinsic Plasticity Is Functionally Altered in Fmr1 KO Cortical Neurons. Cell Rep *26*, 1378-1388 e1373.

Chang, D.T., Honick, A.S., and Reynolds, I.J. (2006). Mitochondrial trafficking to synapses in cultured primary cortical neurons. J Neurosci *26*, 7035-7045.

Chang, D.T., and Reynolds, I.J. (2006). Mitochondrial trafficking and morphology in healthy and injured neurons. Prog Neurobiol *80*, 241-268.

Contractor, A., Klyachko, V.A., and Portera-Cailliau, C. (2015). Altered Neuronal and Circuit Excitability in Fragile X Syndrome. Neuron *87*, 699-715.

Evans, M.D., Sammons, R.P., Lebron, S., Dumitrescu, A.S., Watkins, T.B., Uebele, V.N., Renger, J.J., and Grubb, M.S. (2013). Calcineurin signaling mediates activity-dependent relocation of the axon initial segment. J Neurosci *33*, 6950-6963.

Grubb, M.S., and Burrone, J. (2010). Activity-dependent relocation of the axon initial segment fine-tunes neuronal excitability. Nature *465*, 1070-1074.

Huber, K.M., Gallagher, S.M., Warren, S.T., and Bear, M.F. (2002). Altered synaptic plasticity in a mouse model of fragile X mental retardation. Proc Natl Acad Sci U S A *99*, 7746-7750.

Khacho, M., Clark, A., Svoboda, D.S., Azzi, J., MacLaurin, J.G., Meghaizel, C., Sesaki, H., Lagace, D.C., Germain, M., Harper, M.E*., et al.* (2016). Mitochondrial Dynamics Impacts Stem Cell Identity and Fate Decisions by Regulating a Nuclear Transcriptional Program. Cell Stem Cell *19*, 232-247.

Kuba, H., Oichi, Y., and Ohmori, H. (2010). Presynaptic activity regulates Na(+) channel distribution at the axon initial segment. Nature *465*, 1075-1078.

Kuzniewska, B., Cysewski, D., Wasilewski, M., Sakowska, P., Milek, J., Kulinski, T.M., Winiarski, M., Kozielewicz, P., Knapska, E., Dadlez, M*., et al.* (2020). Mitochondrial protein biogenesis in the synapse is supported by local translation. EMBO Rep *21*, e48882.

Lee, K.Y., Royston, S.E., Vest, M.O., Ley, D.J., Lee, S., Bolton, E.C., and Chung, H.J. (2015). N-methyl-D-aspartate receptors mediate activity-dependent down-regulation of potassium channel genes during the expression of homeostatic intrinsic plasticity. Mol Brain *8*, 4.

Li, Z., Okamoto, K., Hayashi, Y., and Sheng, M. (2004). The importance of dendritic mitochondria in the morphogenesis and plasticity of spines and synapses. Cell *119*, 873-887.

Licznerski, P., Park, H.A., Rolyan, H., Chen, R., Mnatsakanyan, N., Miranda, P., Graham, M., Wu, J., Cruz-Reyes, N., Mehta, N*., et al.* (2020). ATP Synthase c-Subunit Leak Causes Aberrant Cellular Metabolism in Fragile X Syndrome. Cell *182*, 1170-1185 e1179.

Meredith, R.M., Holmgren, C.D., Weidum, M., Burnashev, N., and Mansvelder, H.D. (2007). Increased threshold for spike-timing-dependent plasticity is caused by unreliable calcium signaling in mice lacking fragile X gene FMR1. Neuron *54*, 627-638.

Muddashetty, R.S., Nalavadi, V.C., Gross, C., Yao, X., Xing, L., Laur, O., Warren, S.T., and Bassell, G.J. (2011). Reversible inhibition of PSD-95 mRNA translation by miR-125a, FMRP phosphorylation, and mGluR signaling. Mol Cell *42*, 673-688.

Muraro, N.I., Weston, A.J., Gerber, A.P., Luschnig, S., Moffat, K.G., and Baines, R.A. (2008). Pumilio binds para mRNA and requires Nanos and Brat to regulate sodium current in Drosophila motoneurons. J Neurosci *28*, 2099-2109.

Niere, F., Wilkerson, J.R., and Huber, K.M. (2012). Evidence for a fragile X mental retardation protein-mediated translational switch in metabotropic glutamate receptor-triggered Arc translation and long-term depression. J Neurosci *32*, 5924-5936.

Nobile, V., Palumbo, F., Lanni, S., Ghisio, V., Vitali, A., Castagnola, M., Marzano, V., Maulucci, G., De Angelis, C., De Spirito, M*., et al.* (2020). Altered mitochondrial function in cells carrying a premutation or unmethylated full mutation of the FMR1 gene. Hum Genet *139*, 227-245.

Osterweil, E.K., Krueger, D.D., Reinhold, K., and Bear, M.F. (2010). Hypersensitivity to mGluR5 and ERK1/2 leads to excessive protein synthesis in the hippocampus of a mouse model of fragile X syndrome. J Neurosci *30*, 15616-15627.

Rangaraju, V., Lauterbach, M., and Schuman, E.M. (2019). Spatially Stable Mitochondrial Compartments Fuel Local Translation during Plasticity. Cell *176*, 73-84 e15.

Rath, S., Sharma, R., Gupta, R., Ast, T., Chan, C., Durham, T.J., Goodman, R.P., Grabarek, Z., Haas, M.E., Hung, W.H.W*., et al.* (2021). MitoCarta3.0: an updated mitochondrial proteome now with sub-organelle localization and pathway annotations. Nucleic Acids Res *49*, D1541-D1547.

Richter, J.D., Bassell, G.J., and Klann, E. (2015). Dysregulation and restoration of translational homeostasis in fragile X syndrome. Nat Rev Neurosci *16*, 595-605.

Shen, M., Wang, F., Li, M., Sah, N., Stockton, M.E., Tidei, J.J., Gao, Y., Korabelnikov, T., Kannan, S., Vevea, J.D*., et al.* (2019). Reduced mitochondrial fusion and Huntingtin levels contribute to impaired dendritic maturation and behavioral deficits in Fmr1-mutant mice. Nat Neurosci *22*, 386-400.

Soden, M.E., and Chen, L. (2010). Fragile X protein FMRP is required for homeostatic plasticity and regulation of synaptic strength by retinoic acid. J Neurosci *30*, 16910-16921.

Suhl, J.A., Chopra, P., Anderson, B.R., Bassell, G.J., and Warren, S.T. (2014). Analysis of FMRP mRNA target datasets reveals highly associated mRNAs mediated by G-quadruplex structures formed via clustered WGGA sequences. Hum Mol Genet *23*, 5479-5491.

Sutton, M.A., Ito, H.T., Cressy, P., Kempf, C., Woo, J.C., and Schuman, E.M. (2006). Miniature neurotransmission stabilizes synaptic function via tonic suppression of local dendritic protein synthesis. Cell *125*, 785-799.

Turrigiano, G.G., Leslie, K.R., Desai, N.S., Rutherford, L.C., and Nelson, S.B. (1998). Activity-dependent scaling of quantal amplitude in neocortical neurons. Nature *391*, 892-896.

Valenti, D., de Bari, L., De Filippis, B., Henrion-Caude, A., and Vacca, R.A. (2014). Mitochondrial dysfunction as a central actor in intellectual disability-related diseases: an overview of Down syndrome, autism, Fragile X and Rett syndrome. Neurosci Biobehav Rev *46 Pt 2*, 202-217.

Weisz, E.D., Towheed, A., Monyak, R.E., Toth, M.S., Wallace, D.C., and Jongens, T.A. (2018). Loss of Drosophila FMRP leads to alterations in energy metabolism and mitochondrial function. Hum Mol Genet *27*, 95-106.

Wiemerslage, L., and Lee, D. (2016). Quantification of mitochondrial morphology in neurites of dopaminergic neurons using multiple parameters. J Neurosci Methods *262*, 56-65.

Figures

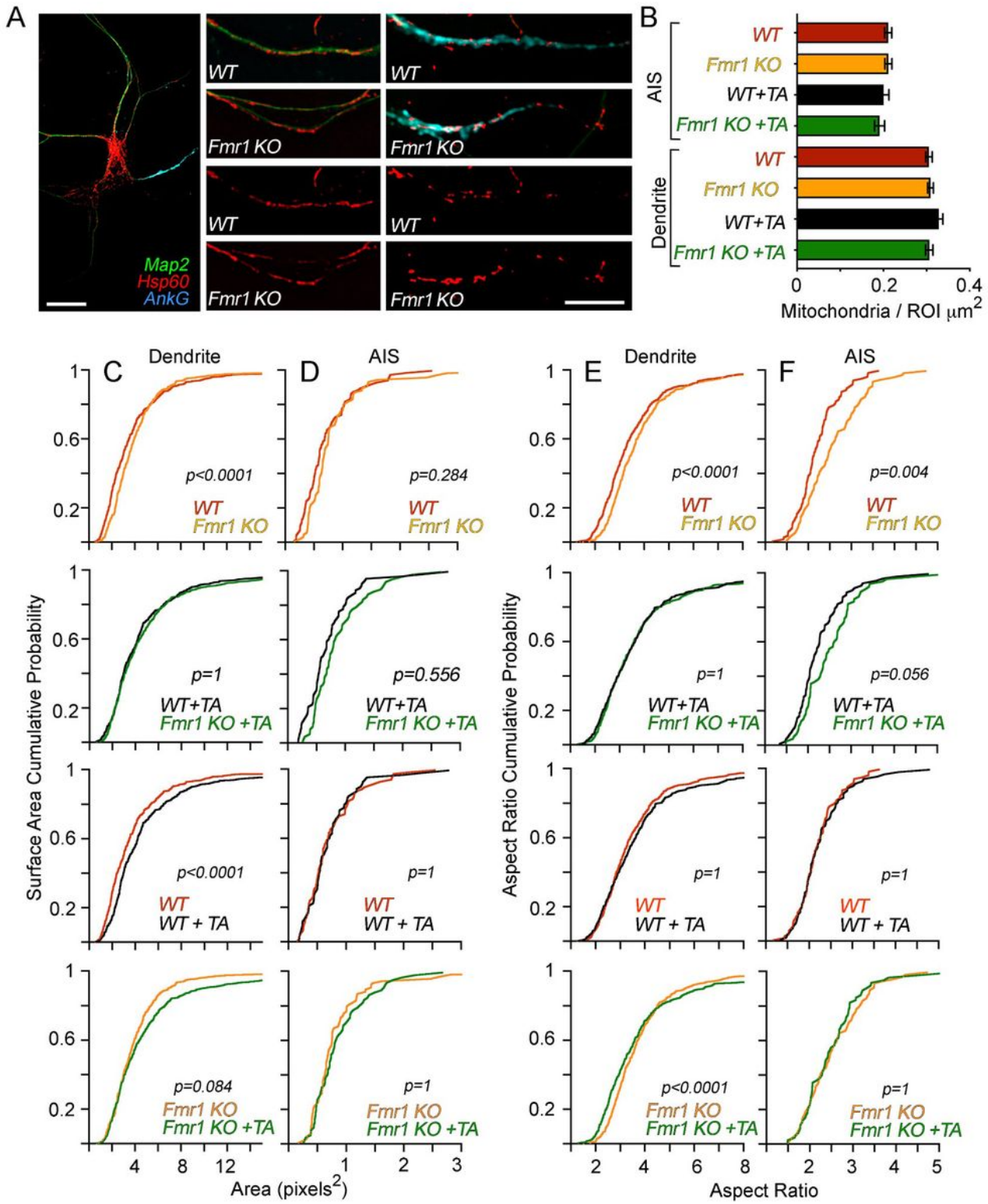

Figure 1

Genotype specific, compartment specific and treatment specific alterations in mitochondria! morphology. A) Representative images of immunofluorescence co-labeling of Hsp60, Map2 and Ank G. Scale bars = 20 microns. From left: full neuron, dendrite, AIS. B) Quantification of mitochondria content in dendrites

and AIS. There were no differences in content of mitochondria between any conditions. Error bars represent the standard error of the mean. C) Quantification and comparison of dendritic mitochondria! surface area before and after TTX/APV treatment. At baseline, mitochondria display significantly larger surface area in Fmr1 KO compared to WT. TTX/APV increases mitochondria! surface area in WT dendrites. Fmr1 KO mitochondria display a non-significant trend towards an increase of surface area following TTX/APV. D) Quantification and comparison of AIS mitochondria) surface area before and after TTX/APV treatment. There are no differences in surface area between any conditions before or after TTX/APV. E) Quantification and comparison of dendritic mitochondria! aspect ratio between genotypes before and after TTX/APV treatment. At baseline, the mitochondria! aspect ratio is increased in Fmr1 KO neurons, but this difference is abolished after TTX/APV. Interestingly, Fmr1 KO mitochondria display a small but significant increase in the aspect ratio after TTX/APV, while no changes occur in the WT. F) Quantification and comparison of AIS residing mitochondria! aspect ratio before and after TTX/APV treatment. At baseline, mitochondria display increased aspect ratio in Fmr1 KO AIS compared to WT, but this difference is lost after TTX/APV treatment. All figures represent data from N = 3 biological replicates from independent littermate culture sets. Each analyzed dendrite and AIS represents an individual data point. N of analyzed dendrites: WT n=400, Fmr1 KO n=427, WT + TA n=366, Fmr1 KO + TA n=377. N of AIS: WT n=90, Fmr1 KO n=80, WT + TA n=74, Fmr1 KO + TA n=69. TA = TTX/APV.

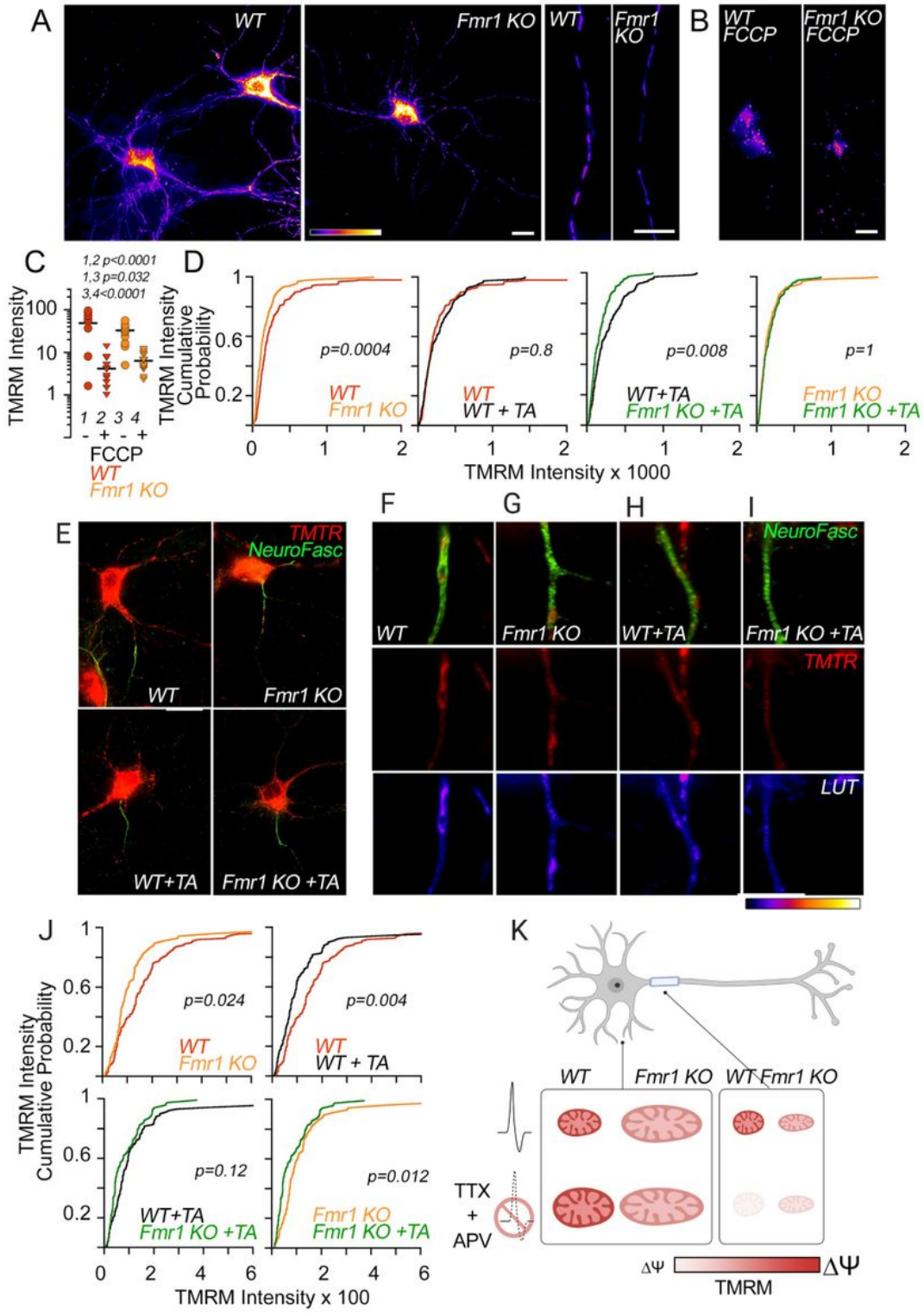

Figure 2

Compartmentalized membrane potential modifications in WT and Fmr1 KO mitochondria before and after activity deprivation. A) Representative images of TMRM labeled neurons. Scale bars = 20 microns. From left: full neurons either in control conditions or after FCCP (0.5 uM) treatment, representative dendritic segments. B+C) FCCP treatment caused significantly reduced TMRM signals in dendritic mitochondria of both WT (1,2) and Fmr1 KO (3,4); + = FCCP, - = no FCCP. D) TMRM intensity is

significantly reduced in dendrites of Fmr1 KO compared to WT at baseline and after TTX/APV treatment. TMRM signal in dendrites was not affected by TTX/APV treatment in either genotype. E) Representative images of co-labeled neurons with TMRM and AIS specific marker Neurofascin from all conditions. F-I) Top: Representative images of Neurofascin positive neurites co-localizing with TMRM-labeled mitochondria. Middle: Same neurite segment as in top row but with Neurofascin stain removed to isolate the co-localizing TMRM labeled mitochondria. Bottom: Same images as above but pseudo-colored according to TMRM-label fluorescence intensity. Row F = WT, G = Fmr1 KO, H = WT + TTX/APV, I = Fmr1 KO + TTX/APV. J) At baseline, AIS residing Fmr1 KO mitochondria display significantly reduced TMRM-intensity. Following TTX/APV, mitochondria in the AIS significantly reduce their TMRM signal in both genotypes. However, the TTX/APV induced reduction in TMRM signal is of greater magnitude in the wild type compared to Fmr1 KO. N of analyzed dendrites: wild type n=210, Fmr1-/y n=175, wild type treated with TTX-APV n=179, Fmr1-/y treated with TTX-APV n=187. N of AIS: WT n=75, Fmr1 KO n=62, WT + TA n=67, Fmr1 KO + TA n=59. K) Summary Model: Compartment specific regulation of mitochondria morphology and polarization by FMRP and activity deprivation. After TTX/APV, WT mitochondria are enlarged in the dendrites and depolarized in the AIS. At baseline, Fmr1 KO neurons present with enlarged and/or elongated mitochondria in the dendrite and AIS, respectively, and mitochondria in both compartments display depolarized membrane potential. After TTX/APV, Fmr1 KO mitochondria do not show changes in their size, and only a slight further reduction in polarization. TA = TTX/APV